Electronic Supplementary Information

Graphene Quantum Dots against Human IAPP Aggregation and Toxicity in Vivo

Miaoyi Wang,[†¶] Yunxiang Sun,[£] Xueying Cao,[‡] Guotao Peng,[¶] Ibrahim Javed,[†] Aleksandr Kakinen,[†]

Thomas P. Davis,[†*] Sijie Lin,[¶*] Jingquan Liu,[‡*] Feng Ding,[£*] Pu Chun Ke[†*]

[†]ARC Centre of Excellence in Convergent Bio-Nano Science and Technology, Monash Institute of Pharmaceutical Sciences, Monash University, 381 Royal Parade, Parkville, VIC 3052, Australia

[¶¶]College of Environmental Science and Engineering, Biomedical Multidisciplinary Innovation Research Institute, Shanghai East Hospital, Shanghai Institute of Pollution Control and Ecological Security, Key Laboratory of Yangtze River Water Environment, Ministry of Education, Tongji University, 1239 Siping Road, Shanghai 200092, China

[£]Department of Physics and Astronomy, Clemson University, Clemson, SC 29634, USA

[‡]College of Materials Science and Engineering, Institute for Graphene Applied Technology Innovation, Qingdao University, Qingdao 266071, China

Corresponding Authors

[*] Thomas P. Davis: thomas.p.davis@monash.edu; Sijie Lin: lin.sijie@tongji.edu.cn; Jingquan Liu: jliu@qdu.edu.cn; Feng Ding: fding@clemson.edu; Pu Chun Ke: pu-chun.ke@monash.edu.

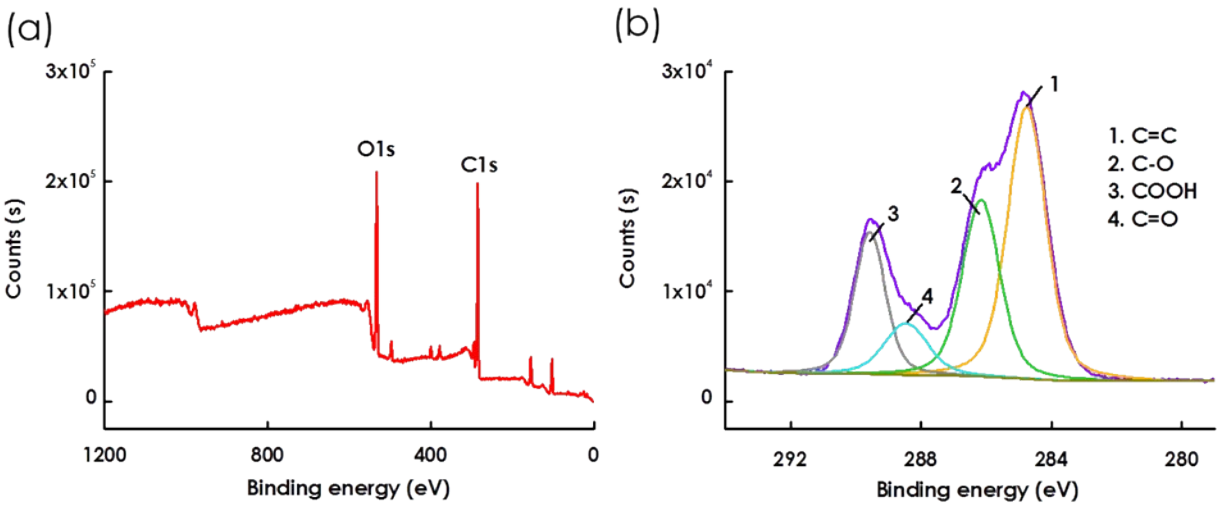

Figure S1. X-ray photoelectron spectroscopy (XPS) was used to monitor the surface composition of GQDs. The two significant peaks corresponded to elemental species C and O in the survey spectra (a). A high-resolution spectrum of C 1s (b) confirmed the presence of C = C (1), C–O (2), COOH (3) and C = O (4) bonds, indicating the as-prepared GQDs were rich in hydroxyl, carbonyl and carboxylic acid groups on their surfaces.

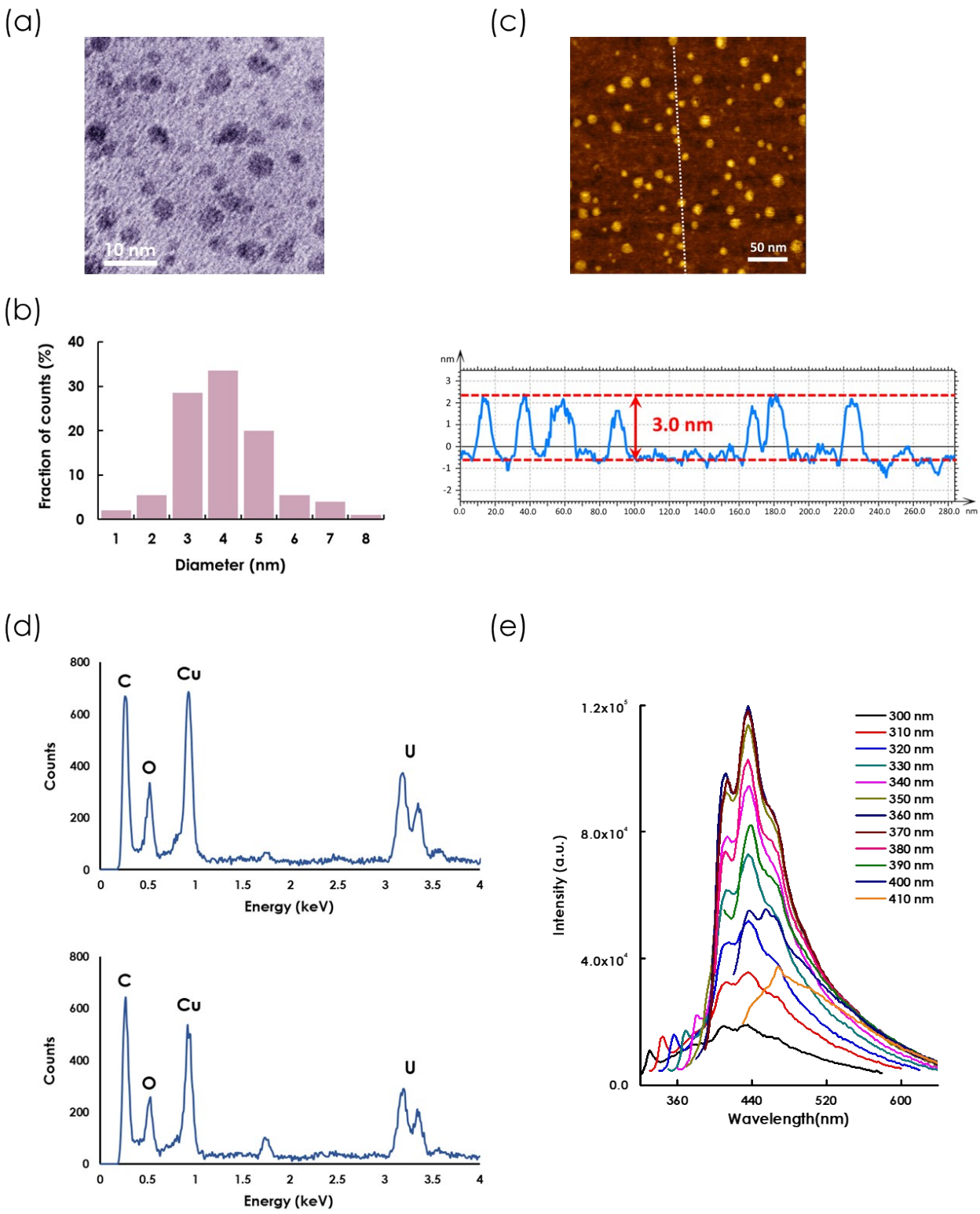

Figure S2. (a) TEM image of GQDs. (b) Size distribution of GQDs derived from TEM images. (c) AFM image and its corresponding height distribution of GQDs. The relatively large sizes of the GQDs can be attributed to the finite cantilever tip size (7 nm in radius). (d) Representative EDX spectra of GQDs alone (top) and IAPP+GQDs (bottom), in which no traces of impurities were found. Copper (Cu) was originated from TEM grid and Uranium (U) was originated from uranyl acetate staining. (e) Emission spectra of GQDs at specified excitation wavelengths of 300-410 nm.

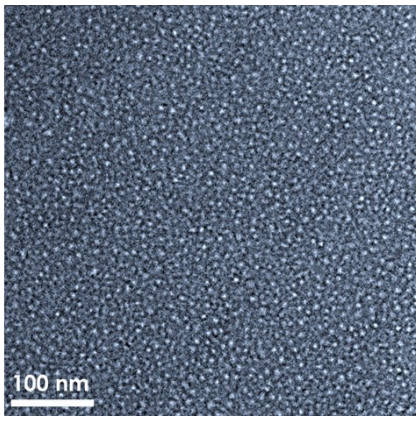

Figure S3. TEM image of IAPP monomers. IAPP concentration: 25 μM.

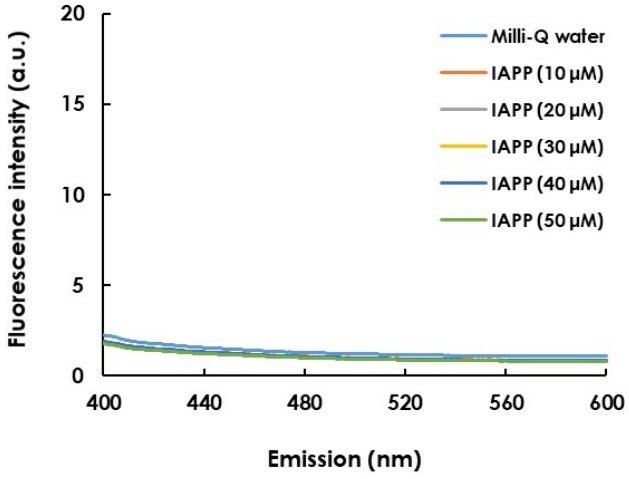

Figure S4. Fluorescence of Milli-Q water and IAPP at different concentrations. Excitation wavelength: 355 nm.

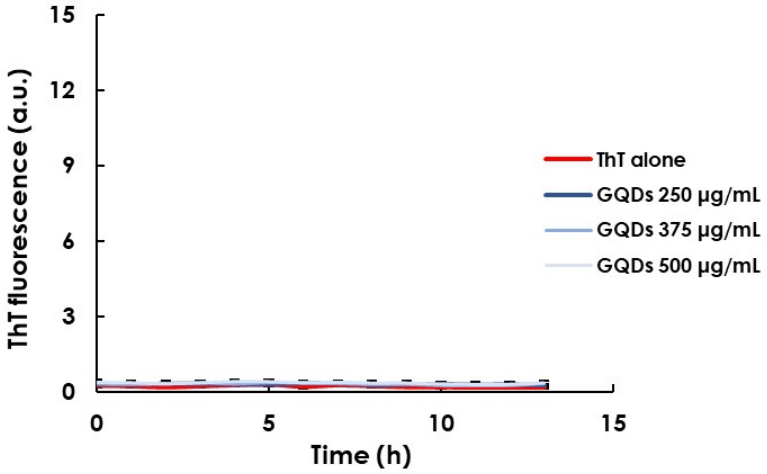

Figure S5. ThT fluorescence of ThT dye alone and GQDs. Excitation wavelength: 440 nm.

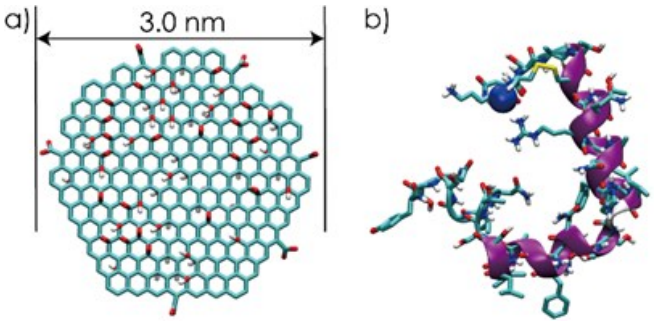

Figure S6. (a) The structure of GQD ($C_{317}O_{81}H_{39}$) and (b) the initial IAPP structure (PDBID: 2L86) used in the simulations.

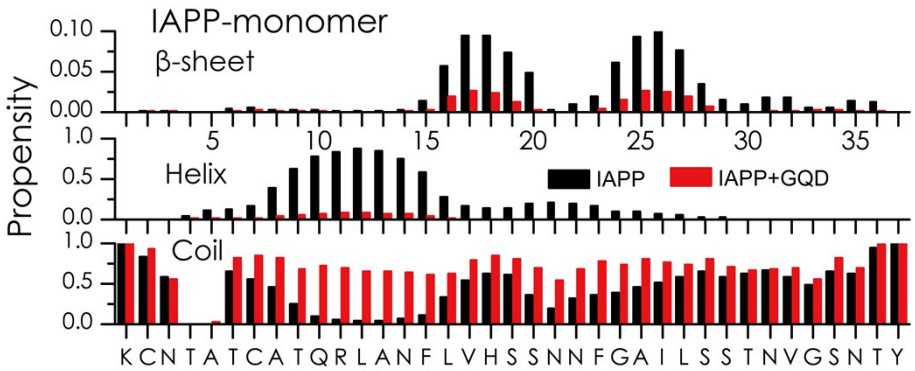

Figure S7. Propensity of each IAPP residue to form β-sheet, helix and coil conformations in IAPP monomer DMD simulations with and without a GQD.

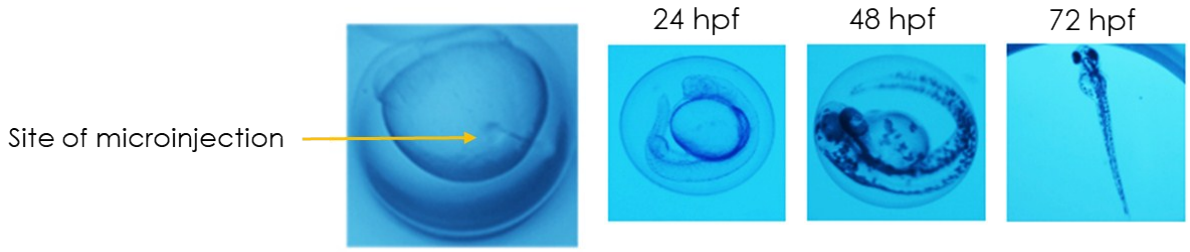

Figure S8. Site of microinjection and development of zebrafish embryos microinjected with H buffer at 24, 48 and 72 hpf.

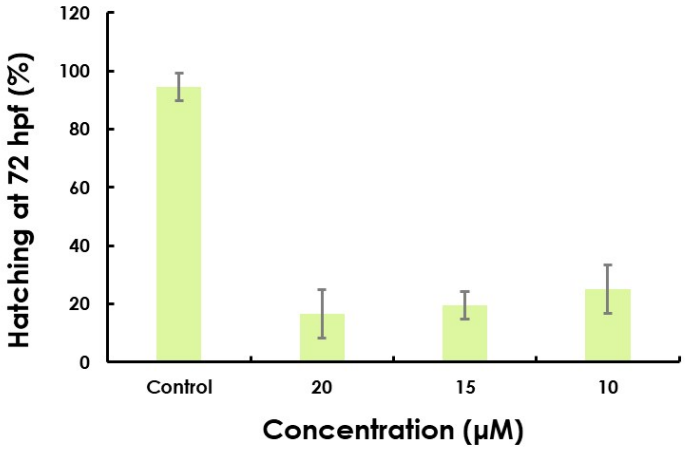

Figure S9. Percentage hatching of zebrafish embryos upon microinjection of IAPP at different concentrations.

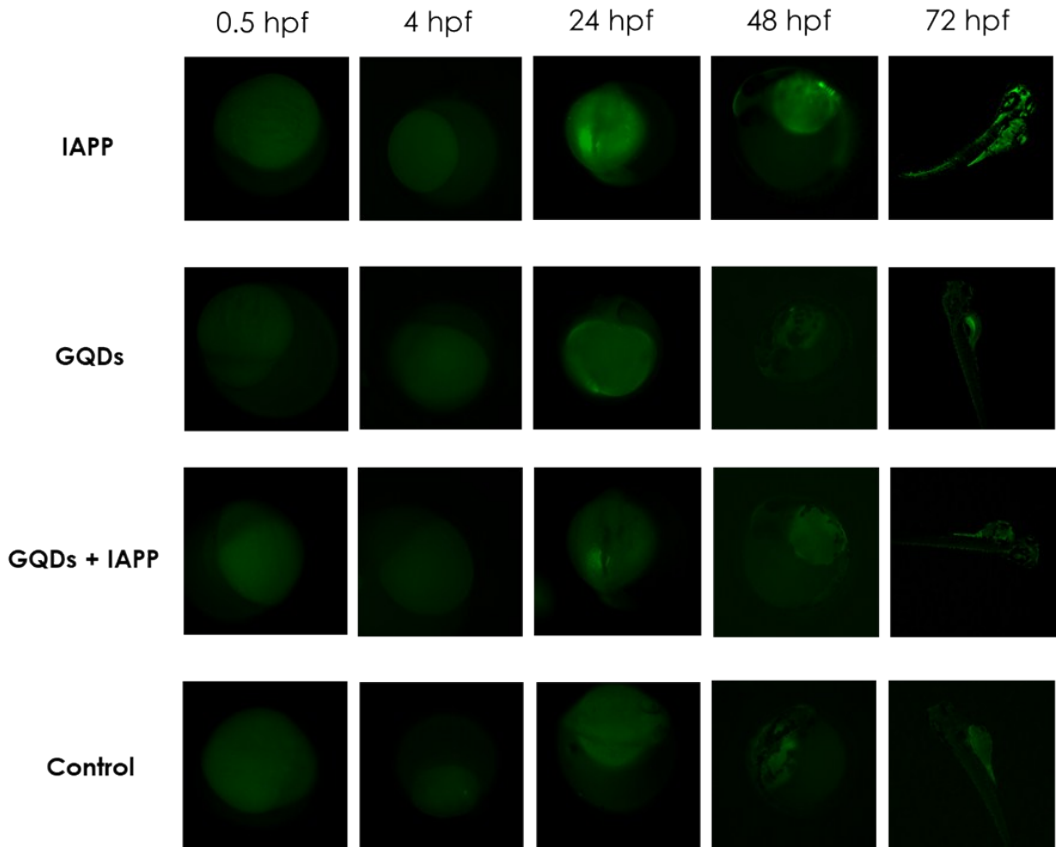

Figure S10. Fluorescence generated from ThT-labelled IAPP cross-β aggregates at 0.5, 4, 24, 48 and 72 hpf using the green fluorescence protein (GFP) channel of a fluorescence microscope. ThT was microinjected together with each sample (IAPP, GQDs, GQDs + IAPP) into the yolk of embryos and ThT microinjected alone was used as control. IAPP concentration: 10 μM. GQD concentration: 150 μg/mL.